

Synchronization of Pancreatic Islet Oscillations by Intrapancreatic Ganglia: A Modeling Study

B. Fendler,^{†*} M. Zhang,[§] L. Satin,[¶] and R. Bertram[†]

[†]Department of Physics and [‡]Department of Mathematics and Programs in Neuroscience and Molecular Biophysics, Florida State University, Tallahassee, Florida; [§]Department of Pharmacology and Toxicology, Virginia Commonwealth University, Richmond, Virginia; and [¶]Department of Pharmacology, and Brehm Diabetes Center, University of Michigan Medical School, Ann Arbor, Michigan

ABSTRACT Plasma insulin measurements from mice, rats, dogs, and humans indicate that insulin levels are oscillatory, reflecting pulsatile insulin secretion from individual islets. An unanswered question, however, is how the activity of a population of islets is coordinated to yield coherent oscillations in plasma insulin. Here, using mathematical modeling, we investigate the feasibility of a potential islet synchronization mechanism, cholinergic signaling. This hypothesis is based on well-established experimental evidence demonstrating intrapancreatic parasympathetic (cholinergic) ganglia and recent *in vitro* evidence that a brief application of a muscarinic agonist can transiently synchronize islets. We demonstrate using mathematical modeling that periodic pulses of acetylcholine released from cholinergic neurons is indeed able to coordinate the activity of a population of simulated islets, even if only a fraction of these are innervated. The role of islet-to-islet heterogeneity is also considered. The results suggest that the existence of cholinergic input to the pancreas may serve as a regulator of endogenous insulin pulsatility *in vivo*.

INTRODUCTION

Plasma insulin levels are pulsatile in normal mice, rats, dogs, and humans (1–4) and this pulsatility is impaired in humans with diabetes (5). In addition, relatives of type II diabetics (6,7) and animal models of human diabetes such as ob/ob mice (8) also show impaired pulsatility. Combined with data showing that pulses of insulin are more efficacious than constant insulin secretion (9–12), this suggests that type II diabetes may be caused, at least in part, by either a loss or irregularity of plasma insulin oscillations.

Insulin secretion from isolated islets is pulsatile because of electrical bursting oscillations. In an islet, the individual insulin-secreting β -cells coordinate their bursting activity primarily through gap junctions. During a burst of electrical impulses the Ca^{2+} concentration in the cytosol rises, evoking insulin secretion (13). The period of the slow electrical and Ca^{2+} oscillations in the islet, which is 5–7 min (14–18), is similar to the period of insulin oscillations measured in plasma *in vivo* (2,3,17,19). Since the insulin in plasma is oscillatory and the islets produce insulin oscillations of a similar frequency, a substantial fraction of the islets must therefore be synchronized, otherwise no oscillation in the blood insulin level would be observed (15,21).

To mediate this synchronization, a number of potential mechanisms have been proposed. One is mutual feedback between the pancreas and liver. Insulin secretion from islets promotes glucose absorption by the liver, affecting all islets. This has a synchronizing effect on the islet population, as was demonstrated in a recent computational study (22). However, this mechanism cannot explain results from

in vitro experiments showing that insulin released from perfused pancreas also oscillates (23,24). Another potential synchronizing mechanism is neural input from intrapancreatic ganglia (25). There is a rich innervation of the pancreas by preganglionic vagal neurons (26–29). These autonomic nerves synapse onto intrapancreatic ganglia—clusters of neurons that are spread in a connective plexus throughout the pancreas in rat, cat, rabbit, guinea pig, and mouse (30–33). The ganglia have been shown to be electrically excitable when autonomic nerve trunks are stimulated in cat (31). Furthermore, *in vitro* and *in vivo* vagal stimulation promotes glucose-dependent insulin release from the pancreas (28,34–36). Ganglia are often found in the proximity of islets and provide innervation (30,37,38). On the receiving end, β -cells express muscarinic receptors (39,40) and neurons in the pancreatic ganglia of rat, cat, rabbit, and guinea pigs express choline acetyltransferase (30,41). In addition, intrahepatic transplantation of islets to diabetic rats only results in peripheral insulin pulsatility after a 200-day lag (42). This delay may reflect the time required for reinnervation of the islets and thus the synchronization of their activity.

Our goal in this computational study was to investigate the feasibility of the hypothesis that cholinergic neural ganglia can serve as an islet-synchronizing agent and to assess the consequences of periodic neuronal activity on endogenous islet insulin pulsatility.

To this end, we used a mathematical model of the β -cell, the dual oscillator model (DOM), which has been shown to reproduce many of the essential behaviors of the pancreatic islet (43,44). The model is composed of two oscillatory subsystems. The first is an electrical subsystem, which produces fast bursts of action potentials and also accounts for changes in the free Ca^{2+} concentration of the cell. The second

Submitted January 23, 2009, and accepted for publication May 8, 2009.

*Correspondence: bfendler@sb.fsu.edu or bfendler@mailier.sb.fsu.edu

Editor: Robert Hsiu-Ping Chow.

© 2009 by the Biophysical Society

0006-3495/09/08/0722/8 \$2.00

doi: 10.1016/j.bpj.2009.05.016

oscillatory component includes β -cell glycolysis, where feedback onto the allosteric enzyme phosphofructokinase (PFK) leads to metabolic oscillations (21,45–47). The glycolytic oscillation drives the slow component of the model cell's oscillation, through effects of ATP and ADP on ATP-sensitive K^+ ion channels in the electrical subsystem.

We have recently shown experimentally that a single large bolus of the muscarinic agonist carbachol (ACh) can synchronize a population of mouse islets *in vitro* (48). The islets remain synchronized for many minutes after agonist application, but eventually drift apart. In accompanying computer simulations, we found that a population of islets modeled by the DOM produced a similar synchronizing response. The islet studies are consistent with previous findings that ACh or carbachol pulses initiate Ca^{2+} oscillations in β -cells and β -cell aggregates (49,50). According to our model, the carbachol pulse leads to the release of Ca^{2+} from the endoplasmic reticulum (ER), resulting in a transient increase in the cytosolic Ca^{2+} concentration. The pumping of cytosolic Ca^{2+} from the cell or into the ER utilizes ATP, lowering β -cell ATP levels. Since ATP inhibits PFK, the resulting drop in the cytoplasmic ATP concentration transiently increases PFK activity. This perturbation to the glycolytic oscillator, applied simultaneously to all islets in the chamber, resets the oscillators to the same phase, thus synchronizing them. The novelty of this method of synchronization is that the slow glycolytic oscillations driving the membrane potential can be synchronized through ACh pulses, even though the muscarinic pathway has no direct effect on glycolysis. We emphasize that ACh pulses in the model result in the synchronization of the collection of islets but are not required for oscillations of individual islets to occur. The latter process is endogenous to the islet due to mechanisms that reflect the ionic and metabolic dynamics of the β -cells.

In this computational study, we simulated agonist pulses of a much smaller and more physiological magnitude to determine whether periodic pulsing can synchronize the model islets. This periodic pulsing is representative of what could be produced by the neural ganglia (31). In the first section, we investigate the effect of a large single agonist pulse and discuss similarities between the model results and experimental data (48). Next, we investigate the effects of continuous pulsing of the DOM and 1), determine whether the driver of the model slow oscillations, glycolysis, can be entrained to periodic ATP levels and 2), determine whether it is possible to synchronize a population of islets with heterogeneous frequencies. Finally, we investigate what fraction of model islets must be innervated to yield coherent insulin oscillations.

MATERIALS AND METHODS

The mathematical model

We used the three-compartment model developed by Bertram et al. (44). The first compartment describes glycolysis, which can generate an independent slow oscillation. The second compartment models mitochondrial metabo-

lism. The third compartment describes plasma membrane electrical activity and cytoplasmic Ca^{2+} handling. Complete mathematical and physical descriptions of the model can be found in Bertram et al. (44).

The glycolytic oscillator component models the M-type (muscle-type) isoform of PFK that results in oscillatory glycolysis in muscle extracts (21,45). PFK is an allosteric enzyme (Fig. 1) whose catalytic rate is affected by different metabolites, including adenosine monophosphate, adenosine triphosphate (ATP), fructose 6-phosphate, and fructose 1, 6-bisphosphate (FBP). The enzymatic product of PFK, FBP, accelerates PFK activity whereas subsequent substrate depletion decelerates it, leading to oscillations. ATP is an inhibitor of PFK. As glucose 6-phosphate is in rapid equilibrium with fructose 6-phosphate, both are representative of the levels of PFK substrate. As originally modeled by Smolen (51), the glycolytic cycle is described by

$$\frac{d(G6P)}{dt} = (J_{GK} - J_{PFK}), \quad (1)$$

$$\frac{d(FBP)}{dt} = \left(J_{PFK} - \frac{1}{2}J_{GPDH} \right), \quad (2)$$

where J_{GK} is the glucokinase reaction rate, J_{PFK} is the PFK reaction rate, and J_{GPDH} is the glyceraldehyde 3-P dehydrogenase reaction rate, which is a surrogate for the later steps of glycolysis. Functional forms and further descriptions of the rates can be found in Bertram et al. (44). In this model, FBP feedback is central in generating oscillations through acceleration of the PFK reaction rate. Importantly, the model does not depend on ATP directly for producing the oscillations, but ATP can terminate the oscillations if its concentration becomes either too high or too low. This was demonstrated previously where membrane hyperpolarization terminated glycolytic oscillations by elevating the cytosolic ATP concentration (44). The opposite occurs in response to muscarinic activity. In this case, IP_3 formed in response to the occupation of muscarinic receptors and G-protein

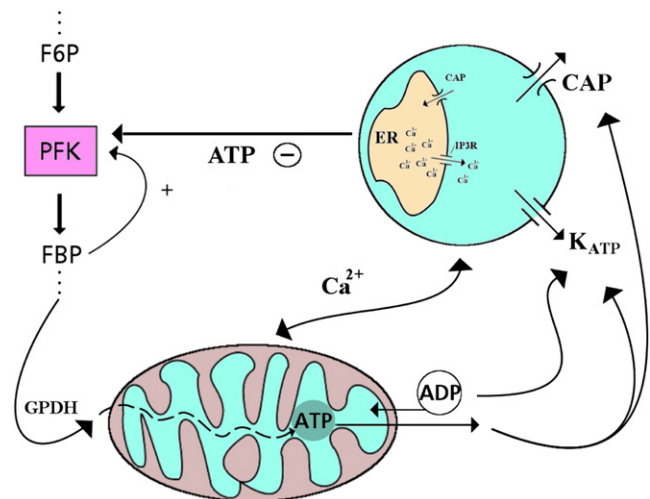


FIGURE 1 This figure demonstrates the feedback between each component in the β -cell model. (Top left) Glycolytic component: cytosolic FBP concentration promotes PFK activity while inhibition arises from increasing ATP levels. In our model, ATP-induced PFK inhibition is the pathway through which muscarinic stimulation results in synchronization. (Top right) Electrical/calcium component: $K(ATP)$ ion channel open probability is affected by ADP and ATP levels. When ATP levels are reduced sufficiently, the islet hyperpolarizes. Ca^{2+} -ATPase pumps (CAP) shuttle Ca^{2+} from the cytosol at the expense of ATP. (Bottom) Mitochondrial component: glycolysis produces pyruvate (model assumes FBP ends in pyruvate production) that feeds into the mitochondria and fuels the oxidative production of ATP from ADP.

mediated phospholipase C (PLC) activation results in the release of Ca^{2+} from the endoplasmic reticulum (ER). Consequently, the elevation of cytosolic Ca^{2+} due to release is cleared by Ca^{2+} -ATPases in the cell. The work done to pump Ca^{2+} utilizes β -cell ATP, lowering its cytosolic concentration. Since ATP inhibits PFK directly, increasing Ca^{2+} pump activity links cell electrical activity (via Ca^{2+}) to glycolysis.

When studying the glycolytic component in isolation we apply a sinusoidal ATP forcing function,

$$ATP = ATP_0 + A \sin(\omega t), \quad (3)$$

where ATP_0 is the mean concentration of ATP, A is forcing function amplitude, and ω is the frequency of the oscillation. This function provides a rough description of periodic pulsing produced by the neural ganglia. A more physiological, periodic square-wave forcing function was also investigated, but the results were similar and are thus not shown.

To study the effects of ACh on the full model, an electrical compartment must be included. The equations describing this compartment are modeled as in previous articles (43,44). The compartment includes voltage and activation variables for K^+ and Ca^{2+} ion channels, the cytosolic and ER Ca^{2+} concentrations, and the cytosolic ADP concentration. No modifications have been made to equations used previously to describe these variables, except where noted. The free Ca^{2+} concentrations are described as

$$\frac{dCa_c}{dt} = f_c(J_{\text{mem}} + J'_{\text{er}} + \kappa J_m), \quad (4)$$

$$\frac{dCa_{\text{er}}}{dt} = -f_{\text{er}}(V_c/V_{\text{er}})J'_{\text{er}}, \quad (5)$$

where Ca_c and Ca_{er} are the free Ca^{2+} concentrations of the cytosol and ER, respectively; f_c and f_{er} are the fractions of free Ca^{2+} ions in the two compartments; J_{mem} is the flux of Ca^{2+} through the plasma membrane; J_m is the Ca^{2+} flux out of the mitochondria; J'_{er} is the flux out of the ER; and κ is the mitochondria/cytosol volume ratio. When inositol 1, 4, 5-trisphosphate (IP_3) is produced in response to the activation of muscarinic ACh receptors, it binds to IP_3 receptors in the ER membrane, releasing Ca^{2+} into the cytosol (Fig. 1). The only change from Bertram et al. (44) was the addition of a Ca^{2+} flux term J_{IP_3} in J_{er} , so that $J'_{\text{er}} = J_{\text{er}} + J_{\text{IP}_3}$. We used the model of Li and Rinzel (52) for J_{IP_3} , where it is assumed that the activation and inactivation processes are at equilibrium and that all binding steps involving IP_3 and Ca^{2+} are symmetrical. Thus,

$$J_{\text{IP}_3} = \Omega_{\infty}(Ca_{\text{er}} - Ca_c), \quad (6)$$

$$\Omega_{\infty} = \left(\frac{Ca_c}{d_{\text{act}} + Ca_c}\right)^3 \left(\frac{\text{IP}_3}{d_{\text{IP}_3} + \text{IP}_3}\right)^3 \left(\frac{d_{\text{inact}}}{d_{\text{inact}} + Ca_c}\right)^3, \quad (7)$$

where Ω_{∞} is the fraction of open IP_3 receptor/channels, d_{act} , d_{IP_3} , and d_{inact} are constants, and IP_3 is the IP_3 concentration in the cytosol. When the Ca^{2+} concentration in the cytosol rises, insulin secretion is evoked. The following equations were used for insulin secretion,

$$\frac{dI}{dt} = (I_{\infty} - I)/\tau_i, \quad (8)$$

$$I_{\infty} = \left(\frac{Ca_c^2}{Ca_c^2 + K_i^2}\right), \quad (9)$$

where I_{∞} is an increasing, but saturating function of Ca_c . The insulin secretion shown is averaged over 1-min intervals, simulating insulin measurements made in the peripheral circulation.

To test the ability of the ganglia (which innervate the islets (30,37,38)) to synchronize islet-to-islet oscillations, we initially assumed that ganglia contact all of the islets and provided periodic impulse activity. This results in the release of ACh and activation of the β -cell's muscarinic receptors.

TABLE 1 Model parameters

$ATP_0 = 2000 \mu\text{M}$	IP_3 amplitude (single pulse) = $0.333 \mu\text{M}$
$d_{\text{act}} = 0.35 \mu\text{M}$	IP_3 amplitude (train of pulses) = $0.1 \mu\text{M}$
$d_{\text{IP}_3} = 0.5 \mu\text{M}$	IP_3 duration of pulse = 0.5 min
$d_{\text{inact}} = 0.4 \mu\text{M}$	$\tau_i = 1 \text{ s}$, $K_i = 0.15 \mu\text{M}$

Muscarinic activation occurs through the G_q pathway to promote IP_3 production via PLC. Thus, we modeled ganglionic input to the collection of islets as a periodic IP_3 square-wave function, using the parameters listed in Table 1.

Communication between the different compartments is key to synchronization of the model islets. The output of glycolysis provides the input to the mitochondrial compartment where the bulk of the ATP is produced. Mitochondria produce ATP at the expense of ADP (Fig. 1), which can influence PFK activity. The mitochondrion's inner membrane potential is affected by Ca^{2+} flux across the membrane, and some dehydrogenases are stimulated by Ca^{2+} . The mitochondria communicate with the plasma membrane through the actions of ATP and ADP on K(ATP) potassium ion channels (53,54).

Differential equations were solved numerically with the explicit adaptive Dormand Prince eighth-order integrator with a tolerance of 10^{-9} , implemented in the XPPAUT software package (55). Other programs were written in C++ to implement iterative XPPAUT models and analyze the resultant frequencies. The analysis programs, some of which employed the software package FFTW (56) in Linux and Cygwin distributions, were used to generate the Arnold tongue and devil staircase diagrams. All XPPAUT programs can be downloaded freely from <http://www.math.fsu.edu/~bertram/software/islet>.

Cytosolic Ca^{2+} measurements

Measurements of intracellular $[\text{Ca}^{2+}]$ oscillations from multiple islets were carried out as in Zhang et al. (48). Briefly, islets from Swiss-Webster mice were loaded with $5 \mu\text{mol/L}$ fura-2/AM and the $340 \text{ nm}/380 \text{ nm}$ fluorescence ratio was measured using an inverted epifluorescence microscope (model No. IX-50; Olympus, Tokyo, Japan) and dual ratio imaging system (Scanalytics, Ft. Lauderdale, FL). Fluorescence ratios were determined from three or more islets simultaneously. Recordings were made at $32\text{--}35^\circ\text{C}$ in a 1 mL recording chamber that was continuously perfused at 1 mL/min at 11.1 mM glucose.

RESULTS

A single, large amplitude pulse of IP_3 transiently synchronizes model islets

In a previous report, we found that a single, large pulse of IP_3 was able to synchronize a population of model islets. This was consistent with our experimental data showing synchronization in response to a large bolus of the muscarinic agonist carbachol (48). In the model, the synchronization produced was due to a “ringing” or damped oscillator phenomenon. When the model islets were exhibiting ringing, the period of the resulting oscillation was less than before the IP_3 pulse occurred. However, such a change in period was not observed in the experimental data—suggesting that this mechanism may not be responsible for islet synchronization.

We have subsequently found that by reducing the maximum conductance of the K(ATP) current from $g_{\text{K(ATP)}} = 16,000 \text{ pS}$ to $12,600 \text{ pS}$, transient synchronization

can also be achieved but without ringing or a decrease in period. This is shown in Fig. 2 A. Before the IP_3 pulse the model islets, which have identical individual properties, are out of phase. An IP_3 pulse of 0.5 min duration occurs at $t = 35$ min resulting in a large release of Ca^{2+} from the ER, which floods the cytosol with Ca^{2+} (*i*). The cytosolic Ca^{2+} is quickly cleared and then a brief, slow oscillation (*ii*), followed by a long silent phase (*iii*), are seen. After this (at $\sim t = 40$ min), an extra-long burst occurs (*iv*). Subsequently, the islets return to their normal oscillatory behavior and remain synchronized, which is expected, because they are identical islets. There is some drift observed due to the chaotic nature of the system when $g_{K(\text{ATP})} = 12,600$ pS.

Similar experimental results are seen when islets are infused with a 15-s pulse of carbachol (Fig. 2 B). In particular, note the transient response which occurs following the carbachol application (here, carbachol is a surrogate for IP_3), from $t = 35$ – 50 min. There is an initial sharp rise in Ca^{2+} due to Ca^{2+} release from the ER (*i*) and very shortly afterwards, a fast compound burst begins at $\sim t = 36$ min (*ii*). Then, a long silent phase occurs (*iii*) followed by an extra-long burst starting at $\sim t = 40$ min (*iv*). After the burst, the islets remain synchronized for the remainder of the recording period. It is clear from Fig. 2 that the model prediction, which is a direct consequence of the glycolytic oscillations, well reproduces the experimentally observed islet response to carbachol application.

A train of small-amplitude IP_3 pulses also generates long-lasting synchronization

We next turn to what we would expect to represent a more physiologically relevant form of long-term synchronization consisting of periodic neuronal input to a collection of model

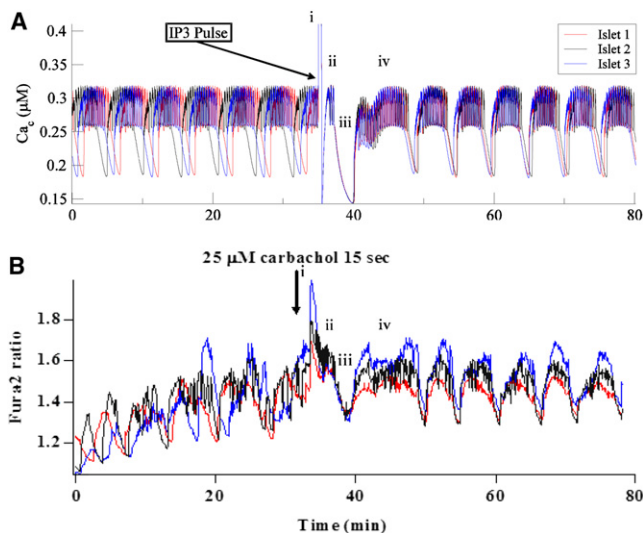


FIGURE 2 (A) Single large IP_3 pulse synchronizes three identical model islets. (B) A 15 s application of the muscarinic agonist carbachol synchronizes three islets in 11.1 mM glucose. Ca^{2+} concentration is measured through the Fura2 ratio.

islets. In Fig. 2 A, a saturating IP_3 pulse synchronized homogenous model islets. Next, we investigated the possibility that heterogeneous islets may be synchronized by a periodic train of small IP_3 pulses (amplitude of $0.1 \mu\text{M}$). This is more representative of the physiological situation where a large number of islets are innervated by an intact pancreatic nervous system in vivo than the single large pulse applied in the in vitro experiments (48).

We first attempted to entrain the glycolytic compartment in isolation by periodic input. Since a pulse of IP_3 in the full model ultimately reduces the ATP concentration via ATP hydrolysis by β -cell Ca^{2+} pumps, we simulated the actions of neural input on the glycolytic compartment by episodic reductions of ATP. Fig. 3 shows the FBP concentration observed when pulsed with a periodic train of downward square-wave ATP pulses. Entrainment of the glycolytic model is evident, as for each ATP pulse applied there is a concomitant FBP pulse. We were also interested in other frequency locking ratios, such as 3:2 or 2:1 entrainment. Thus, we systematically varied features of the ATP input function to examine this. For simplicity, we used a sinusoidal ATP function, which was fully characterized by two parameters—amplitude and period. Fig. 4 A shows the so-called devil's staircase for an ATP amplitude (A) of $225 \mu\text{M}$. The diagram shows the winding number (input function period/model response period) plotted as a function of the forcing period. The horizontal line segments indicate period ranges for which the model is entrained to the input function. The primary entrainment region, 1:1 entrainment (*black curve*), was achieved over a wide range of forcing periods, ~ 3 – 10 min. For other input periods, regions of 1:2 (*red*), 1:3 (*green*), 1:4 (*blue*), 1:5 (*yellow*), 2:1 (*cyan*), and 3:2 (*orange*), entrainment are evident.

Fig. 4 B shows an Arnold tongue diagram, which is a summary of all the devil's staircases produced using different forcing amplitudes. Similar results were found using a periodic ATP square wave (not shown). For small amplitudes, the Arnold tongues are triangular. However, for larger amplitudes, the outer edges of the tongues bend, and eventually the 1:1 behavior dominates the entrainment. Between each tongue, the glycolytic model is not entrained.

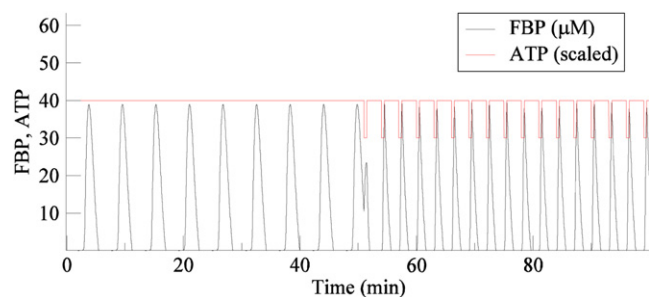


FIGURE 3 Train of periodic ATP pulses (3-min period) entrains the model glycolytic oscillator, which has a natural period of 5.5 min. The ATP time course (*red, top curve*) has been scaled to facilitate comparison with FBP.

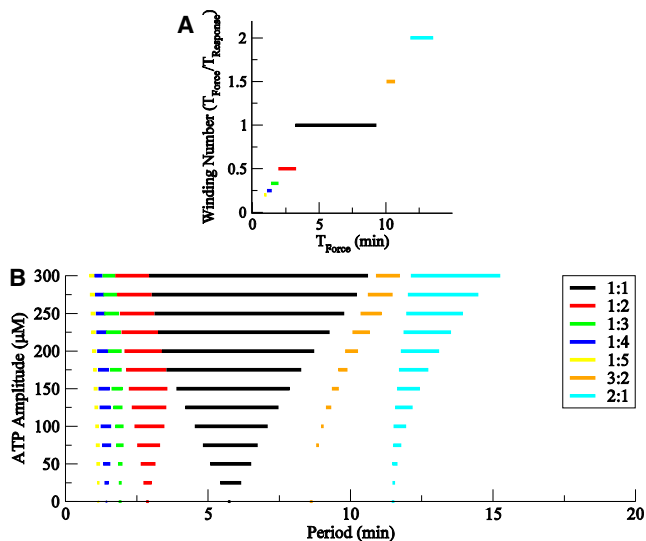


FIGURE 4 (A) Entrainment windows for one amplitude ($A = 225 \mu\text{M}$) of the ATP forcing function. Each bar represents a range of periods for which the glycolytic model is entrained to a sinusoidal oscillation. When the winding number is an integer, or a ratio of two integers for a range of forcing periods, entrainment occurs. (B) Entrainment windows for a range of ATP amplitudes. The points at the $A = 0 \mu\text{M}$ were calculated as fraction multiples of the natural period.

Further, the no entrained regions become smaller as the ATP pulse amplitude is increased. The entrainment bands in the 3:2 Arnold tongue seen below $A = 75 \mu\text{M}$ could not be resolved in our simulations, and thus are not shown. We note that when the periodic pulsing was through glucose application, the insulin oscillations in human islets were shown to be entrainable to 1:1 and 2:1, but in diabetics, 3:1 (57).

We next moved from the glycolytic subsystem alone to the full β -cell model to investigate whether a periodic train of IP_3 pulses can synchronize a population of heterogeneous model islets. Fig. 5 shows pooled, simulated insulin secretion (arbitrary units; black curve) from 51 different model islets, whose natural periods ranged from 3 to 5 min. The heterogeneity in this case was introduced by uniformly varying the glucokinase rate (J_{gk}) from $J_{\text{gk}} = 0.4\text{--}0.5 \mu\text{M/s}$ (the period increased approximately linearly with J_{gk}). Islets were allowed to equilibrate before data collection was commenced.

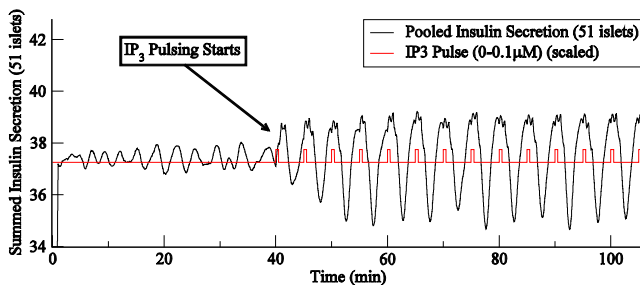


FIGURE 5 Summed insulin secretion from 51 heterogeneous model islets. Once IP_3 pulsing begins, the insulin oscillation increases in magnitude and adopts a regular frequency.

Each islet was subject to the same IP_3 pulse protocol, simulating a ganglionic pacemaker responsible for innervating all islets. IP_3 was zero until $t = 40$ min when pulsing began (red curve). Before $t = 40$ min, the islets were mostly out of phase; although there was some coherence seen in the pooled insulin, the amplitude of the oscillation was small and highly variable. At $t = 40$ min, the IP_3 pulsing began and the pooled insulin exhibited oscillations of growing amplitude as the model islets became progressively synchronized by the applied IP_3 pulsing. It took ~ 20 min for the maximum number of islets to synchronize. As noted earlier, the IP_3 concentration in these simulations was reduced from those in Fig. 2 A. This resulted in smaller reductions of ATP levels, from 0 to $200 \mu\text{M}$, where the saturating pulse resulted in an $\sim 475\text{-}\mu\text{M}$ excursion. In comparison with the Arnold tongues in Fig. 4, a $200\text{-}\mu\text{M}$ reduction of ATP is sufficient to synchronize glycolytic oscillators with natural periods of 3–8 min.

Fig. 6 shows the power spectral density (PSD) obtained using two different IP_3 pulse protocols applied to 51 model islets simulated for 100 min. The red curve shown is the PSD for pooled insulin secretion observed in response to a periodic IP_3 forcing. The PSD has a significant peak at 5 min, demonstrating that a considerable number of insulin-secreting model islets have largely synchronized to the 5 min IP_3 pulse period, despite heterogeneity in the natural periods. The black curve is the PSD of pooled insulin secretion observed for zero IP_3 amplitude (i.e., no IP_3 pulsing applied). Compared to the red curve, the black curve showed little or no frequency dominance with spectral decomposition. Thus, without IP_3 pulsing, the summed insulin time course exhibits no significant dominant frequency, demonstrating that pooled pulsatility does not occur unless the model islets are synchronized.

It is unlikely that the postganglionic cholinergic fibers innervate every islet of the intact pancreas. We thus asked whether a coherent signal, a significant pooled insulin oscillation, could still be observed if only a fraction of the islets received input from the postganglionic neurons of the pancreas. Fig. 7 shows a series of PSDs of pooled insulin observed for different fractions of innervated islets. From inspection of the figure, it appears that all islets need not

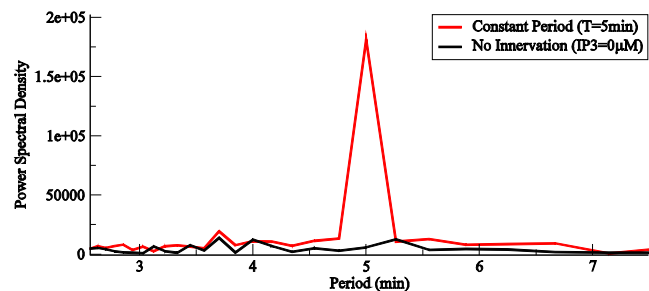


FIGURE 6 Normalized power spectral density of the pooled insulin secretion with (red, upper curve) and without (black, lower curve) periodic IP_3 forcing (amplitude = $0.1 \mu\text{M}$; duration = 0.5 min, period = 5 min).

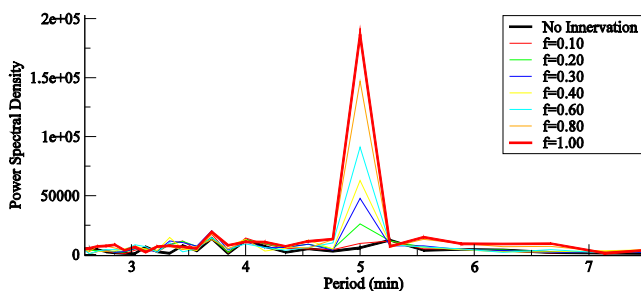


FIGURE 7 Pooled insulin signal from 51 islets is analyzed with different fractions of innervated islets. The PSDs demonstrate that a coherent 5-min insulin oscillation is visible even if only a small fraction of islets is innervated.

be synchronized to produce a significant oscillatory insulin response when compared to no innervation. In fact, even with only 30–40% of islets innervated, a coherent insulin oscillation was observed at the forcing period. This supports the hypothesis that a pulsatile insulin pattern in the peripheral blood can be produced even if only a fraction of the pancreatic islets receives pulsatile input.

The islets were found to synchronize under other IP_3 periods, but due to computational costs we only investigated, in depth, IP_3 periods in the range of 3–5 min. It is reasonable to assume, however, that the islets will synchronize to a larger band of frequencies since glycolysis, the driver of the slow oscillation in the model, entrains to a larger band of ATP frequencies for small ($ATP < 150 \mu M$) ATP amplitudes (Fig. 4). The IP_3 amplitude for the continuous pulse train was chosen to maximize the Ca^{2+} response while minimizing effects on the Ca^{2+} trace. When the IP_3 amplitude was chosen too high, responses such as seen in Fig. 2 resulted. When the amplitude was too low, only weak synchronization occurred.

DISCUSSION

We have shown that a periodic train of acetylcholine pulses can synchronize model islet oscillators driven by glycolytic oscillations. We first showed that it is possible to entrain the glycolytic oscillator with a sinusoidal ATP input function. We then showed that a population of model islets can be synchronized by ACh-induced IP_3 pulses, which lead to downward ATP pulses due to ATP utilization by Ca^{2+} -ATPases. Although the ability to entrain the glycolytic oscillator is necessary for entrainment of the full model, it is not sufficient. The entrainment of the full model occurs through a multisegmented pathway that may not produce sufficient effects on ATP to entrain the oscillator. However, we found that entrainment did occur with a continuous train of IP_3 pulses that only mildly perturbed the Ca^{2+} concentration. Also, assuming that the ACh pulses reflect activity of the pancreatic ganglia, our modeling study showed that it is not necessary for the whole islet population of a pancreas to be innervated to produce a significant oscillatory insulin

response. In fact, only ~35% innervation was required to produce a regular oscillatory insulin signal having a period similar to that measured in vivo in mice (17) and humans (4,57).

Early studies have been performed in canine and human, where either vagotomy or muscarinic antagonists were used to study the effects of cholinergic stimulation on insulin pulsatility. Most of these studies failed to convincingly demonstrate changes in pulsatility (58,59). Other studies showed that the Na^+ channel blocker TTX disrupted plasma insulin pulses (60). Cholinergic agonists (23) and nicotinic antagonists (61) were also effective. In another study, pulsatile insulin from a perfused canine pancreas was examined after muscarinic receptor blockade and after the application of TTX. In both cases, insulin pulsatility persisted, and pulse amplitude even increased after nerve activity was blocked by TTX (61). These results are difficult to understand, since it is hard to reconcile blockage of neural input to islets with an increase in insulin pulsatility from a perfused pancreas. Finally, we note that all of these studies were done on canine or human, rather than on the mouse. There may be species differences in islet synchronization mechanisms (62).

Two previous studies examined the ability of a single pulse of agonist to synchronize clusters of mouse β -cells (63) and islets (48) in vitro. In one study, attempts at synchronizing clusters of β -cells using a 5-min pulse of glucose, amino acids, or the K(ATP) channel blocker tolbutamide (on a background of 12 mM glucose) were unsuccessful (63). In the other study (48), a single tolbutamide pulse of 2-min duration also failed to synchronize β -cells, this time in separate islets rather than in cell clusters. However, in this study brief repolarization with the K(ATP) channel opener diazoxide (2 min pulse) or depolarization with KCl (30 s pulse) did transiently synchronize islets. Most significantly, a single pulse of the muscarinic agonist carbachol consistently produced transient synchronization. It is not evident why brief depolarization with KCl or diazoxide was effective at transiently synchronizing islets whereas depolarization with tolbutamide was not, since in all cases the cytosolic Ca^{2+} concentration would be perturbed. Interestingly, Zarkovic and Henquin (63) showed that a train of tolbutamide pulses was successful at synchronizing β -cell clusters, but in this case the pulses were quite large, so the intrinsic rhythm of the β -cell cluster was disturbed (Fig. 5 of (63)). In the simulations of this article, care was taken to ensure that the magnitude of the pulses in the IP_3 train is sufficiently small so that the endogenous oscillation was only slightly perturbed.

Studies using ATP applied to β -cells and β -cell aggregates in vitro have led to suggestions that synchronization of islets may also occur via a noncholinergic pathway. One set of experiments showed that ATP-induced Ca^{2+} responses in a small population of β -cells (49) occurred, even in the presence of PLC or SERCA pump inhibitors, suggesting that ER Ca^{2+} release due to IP_3 might not be involved (49). However, data arguing against ATP as the sole

synchronizing agent include the demonstration that a population of β -cells can remain synchronized after purinergic receptors are blocked (64), and our own recent data showing that a single large pulse of carbachol synchronizes a small population of islets (48).

Regardless of the detailed mechanism(s) involved in agonist-induced Ca^{2+} transients, our synchronization mechanism only requires that Ca^{2+} -ATPases utilize ATP to pump Ca^{2+} from the cytosol after an initial rise. The change in ATP levels, regardless of the exact cause of the Ca^{2+} changes produced, is what perturbs glycolysis to synchronize the slow oscillations among islets. Therefore, irrespective of the identity of the agent promoting the Ca^{2+} changes, whether it is ACh, extracellular ATP, or other signals, glycolytic flux can be reset and the system synchronized by periodic pulsing. In fact, ACh itself has been shown to directly activate a depolarizing current in the plasma membrane, resulting in Ca^{2+} influx through voltage-dependent Ca^{2+} channels (62). Thus, an ACh pulse increases the cytosolic Ca^{2+} concentration through both store release and Ca^{2+} influx.

Pulsatile insulin secretion has been shown to be more effective on insulin target tissues than a constant, elevated insulin level. Thus, it is likely that nature has designed more than one synchronizing pathway to ensure that pulsatility is preserved in the pancreas. Indeed, this could explain why insulin oscillations have been observed in vivo (1–4,17,57), in perfused pancreas (23,24), and in islet populations (24). In a previous modeling article, we showed that islet interaction with a simple insulin feedback system, which simulated the liver, was also capable of synchronizing a population of islets (22). That is, insulin secreted from the islets induces the liver to store more glucose and release less into the plasma. The resulting reduction in blood glucose concentration acts on all the islets, tending to synchronize their oscillatory activity. This synchronizing influence could complement the synchronizing effects of neural ganglia that we examined in this study.

The goal of our study was to examine the feasibility of a mechanism of islet synchronization that was based on periodic cholinergic input from neurons of intrapancreatic ganglia. The viability of this mechanism was not obvious a priori, since the oscillations in our model islets are driven by oscillations in glycolysis, a biochemical pathway not believed to be directly affected by plasma membrane electrical activity or intracellular Ca^{2+} levels in pancreatic β -cells. We have demonstrated that this novel mechanism is indeed feasible, and it may work alone or in conjunction with other mechanisms to ensure synchronization of oscillations among islets.

It is currently not known whether ganglia neurons are affected by glucose or insulin levels, or what the origin of periodic ganglia activity might be. It is interesting to speculate, however, that if insulin acts on ganglia, then there would be two-way interactions between ganglia and islets. Thus, islets could help set the pacing of ganglion neurons, which, in turn, coordinate islet oscillations.

The authors thank Arthur Sherman, Oliver Steinbock, Bradford Peercy, Pranay Goel, Joel Tabak, Per Arne Rikvold, and the reviewers for helpful suggestions and insight.

Work in the Bertram lab is supported by American Heart Association predoctoral fellowship No. AHA-0715126B and by National Science Foundation grant No. DMS-0613179. M.Z. and L.S. were supported by National Institutes of Health grant No. RO1-DK-46409.

REFERENCES

- Nunemaker, C. S., D. H. Wasserman, O. P. McGuinness, I. R. Sweet, J. C. Teague, et al. 2005. Insulin secretion in the conscious mouse is biphasic and pulsatile. *Am. J. Physiol.* 290:E523–E529.
- Bergsten, P., J. Westerlund, P. Liss, and P. O. Carlsson. 2002. Primary in vivo oscillations of metabolism in the pancreas. *Diabetes.* 51:699–703.
- Porksen, N., S. Munn, J. Steers, J. D. Veldhuis, and P. C. Butler. 1996. Effects of glucose ingestion versus infusion on pulsatile insulin secretion: the incretin effect is achieved by amplification of insulin secretory burst mass. *Diabetes.* 45:1317–1323.
- Song, S. H., S. S. McIntyre, H. Shah, J. D. Veldhuis, P. C. Hayes, et al. 2000. Direct measurement of pulsatile insulin secretion from the portal vein in human subjects. *J. Clin. Endocrinol. Metab.* 85:4491–4499.
- Lang, D. A., D. R. Matthews, M. Burnet, and R. C. Turner. 1981. Brief, irregular oscillations of basal plasma insulin and glucose concentrations in diabetic man. *Diabetes.* 30:435–439.
- O'Rahilly, S., R. C. Turner, and D. R. Matthews. 1988. Impaired pulsatile secretion of insulin in relatives of patients with non-insulin dependent diabetes. *N. Engl. J. Med.* 318:1225–1230.
- Schmitz, O., N. Pørksen, B. Nyholm, C. Skjærbaek, P. C. Butler, et al. 1997. Disorderly and nonstationary insulin secretion in relatives of patients with NIDDM. *Am. J. Physiol.* 272:E218–E226.
- Ravier, M. A., J. Sehlin, and J.-C. Henquin. 2002. Disorganization of cytoplasmic Ca^{2+} oscillations and pulsatile insulin secretion in islets from ob/ob mice. *Diabetologia.* 45:1154–1163.
- Matthews, D. R., B. A. Naylor, R. G. Jones, G. M. Ward, and R. C. Turner. 1983. Pulsatile insulin has greater hypoglycemic effect than continuous delivery. *Diabetes.* 32:617–621.
- Bratusch-Marrain, P. R., M. Komjati, and W. K. Waldhausl. 1986. Efficacy of pulsatile versus continuous insulin administration on hepatic glucose production and glucose utilization in type I diabetic humans. *Diabetes.* 35:922–926.
- Komjati, M., P. Bratusch-Marrain, and W. Waldhausl. 1986. Superior efficacy of pulsatile versus continuous hormone exposure on hepatic glucose production in vitro. *Endocrinology.* 118:312–319.
- Paolisso, G., A. J. Scheen, D. Giugliano, S. Sgambato, A. Albert, et al. 1991. Pulsatile insulin delivery has greater metabolic effects than continuous hormone administration in man: importance of pulse frequency. *J. Clin. Endocrinol. Metab.* 72:607–615.
- MacDonald, P. E., and P. Rorsman. 2007. The ins and outs of secretion from pancreatic β -cells: control of single-vesicle exo- and endocytosis. *Physiology (Bethesda).* 22:113–121.
- Cook, D. L. 1983. Isolated islets of Langerhans have slow oscillations of electrical activity. *Metabolism.* 32:681–685.
- Bergsten, P., E. Grapengiesser, E. Gylfe, A. Tengholm, and B. Hellman. 1994. Synchronous oscillations of cytoplasmic Ca^{2+} and insulin release in glucose-stimulated pancreatic islets. *J. Biol. Chem.* 269:8749–8753.
- Zhang, M., P. Goforth, A. Sherman, R. Bertram, and L. Satin. 2003. The Ca^{2+} dynamics of isolated mouse β -cells and islets: implications for mathematical models. *Biophys. J.* 84:2852–2870.
- Nunemaker, C. S., M. Zhang, D. H. Wasserman, O. P. McGuinness, A. C. Powers, et al. 2005. Individual mice can be distinguished by the period of their islet calcium oscillations: is there an intrinsic islet period that is imprinted in vivo? *Diabetes.* 54:3517–3522.
- Beauvois, M. C., C. Merezak, J.-C. Jonas, M. A. Ravier, and J.-C. Henquin. 2006. Glucose-induced mixed $[\text{Ca}^{2+}]_c$ oscillations in mouse β -cells are

- controlled by the membrane potential and the SERCA3 Ca^{2+} -ATPase of the endoplasmic reticulum. *Am. J. Physiol.* 290:C1503–C1511.
19. Pørksen, N. 2002. The in vivo regulation of pulsatile insulin secretion. *Am. J. Physiol.* 45:E3–E20.
 20. Reference deleted in proof.
 21. Tornheim, K. 1997. Are metabolic oscillations responsible for normal oscillatory insulin secretion? *Diabetes.* 46:1375–1380.
 22. Pedersen, M. G., R. Bertram, and A. Sherman. 2005. Intra- and inter-islet synchronization of metabolically driven insulin secretion. *Biophys. J.* 89:107–119.
 23. Stagner, J. I., E. Samols, and G. C. Weir. 1980. Sustained oscillations of insulin, glucagon, and somatostatin from the isolated canine pancreas during exposure to a constant glucose concentration. *J. Clin. Invest.* 65:939–942.
 24. Sturis, J., W. L. Pugh, J. Tang, D. M. Ostrega, J. S. Polonsky, et al. 1994. Alterations in pulsatile insulin secretion in the Zucker diabetic fatty rat. *Am. J. Physiol.* 267:E250–E259.
 25. Ahren, B. 2000. Autonomic regulation of islet hormone secretion—implications for health and disease. *Diabetologia.* 43:393–410.
 26. Ahren, B., G. J. Taborsky, Jr., and D. Porte, Jr. 1986. Neuropeptidergic versus cholinergic and adrenergic regulation of islet hormone secretion. *Diabetologia.* 29:827–836.
 27. Brunicardi, F. C., D. M. Shavelle, and D. K. Andersen. 1995. Neural regulation of the endocrine pancreas. *Int. J. Pancreatol.* 18:177–195.
 28. Berthoud, H. R., and T. L. Powley. 1990. Identification of vagal preganglionics that mediate cephalic phase insulin response. *Am. J. Physiol.* 258:R523–R530.
 29. Kirchgessner, A. L., and M. D. Gershon. 1990. Innervation of the pancreas by neurons in the gut. *J. Neurosci.* 10:1626–1642.
 30. Coupland, R. E. 1958. The innervation of pancreas of the rat, cat, and rabbit as revealed by the cholinesterase technique. *J. Anat.* 92:143–149.
 31. King, B. F., J. A. Love, and J. H. Szurszewski. 1989. Intracellular recordings from pancreatic ganglia of the cat. *J. Physiol.* 419:379–403.
 32. Kirchgessner, A. L., and J. E. Pintar. 1991. Guinea pig pancreatic ganglia: projections, transmitter content, and the type-specific localization of monoamine oxidase. *J. Comp. Neurol.* 305:613–631.
 33. Ushiki, T., and S. Watanabe. 1997. Distribution and ultrastructure of the autonomic nerves in the mouse pancreas. *Microsc. Res. Tech.* 37:399–406.
 34. Bloom, S. R., and A. V. Edwards. 1980. Pancreatic endocrine responses to stimulation of the peripheral ends of the vagus nerves in conscious calves. *J. Physiol.* 315:31–41.
 35. Ahren, B., and G. J. Taborsky, Jr. 1986. The mechanism of vagal nerve stimulation of glucagon and insulin secretion in the dog. *Endocrinology.* 118:1551–1557.
 36. Nishi, S., Y. Seino, H. Ishida, M. Seno, T. Taminato, et al. 1987. Vagal regulation of insulin, glucagon, and somatostatin secretion in vitro in the rat. *J. Clin. Invest.* 79:1191–1196.
 37. Morgan, C. R., and R. T. Lobl. 1968. A histochemical study of neuro-insular complexes in the pancreas of the rat. *Anat. Rec.* 160:231–237.
 38. Persson-Sjögren, S., A. Zashihin, and S. Forsgren. 2001. Nerve cells associated with the endocrine pancreas in young mice: an ultrastructural analysis of the neuroinsular complex type I. *Histochem. J.* 33:373–378.
 39. Henquin, J.-C., and M. Nenquin. 1988. The muscarinic receptor subtype in mouse pancreatic β -cells. *FEBS Lett.* 236:89–92.
 40. Verspohl, E. J., R. Tacke, E. Mutschler, and G. Lambrecht. 1990. Muscarinic receptor subtypes in rat pancreatic islets: binding and functional studies. *Eur. J. Pharmacol.* 178:303–311.
 41. Liu, M., and A. L. Kirchgessner. 1997. Guinea pig pancreatic neurons: morphology, neurochemistry, electrical properties, and response to 5-HT. *Am. J. Physiol.* 273:G1273–G1289.
 42. Pørksen, N., S. Munn, D. Ferguson, T. O'Brien, J. Veldhuis, et al. 1994. Coordinate pulsatile insulin secretion by chronic intraportally transplanted islets in the isolated perfused rat liver. *J. Clin. Invest.* 94:219–227.
 43. Bertram, R., L. Satin, M. Zhang, P. Smolen, and A. Sherman. 2004. Calcium and glycolysis mediate multiple bursting modes in pancreatic islets. *Biophys. J.* 87:3074–3087.
 44. Bertram, R., L. S. Satin, M. G. Pedersen, D. S. Luciani, and A. Sherman. 2007. Interaction of glycolysis and mitochondrial respiration in metabolic oscillations of pancreatic islets. *Biophys. J.* 92:1544–1555.
 45. Tornheim, K., and J. M. Lowenstein. 1974. The purine nucleotide cycle. IV. Interactions with oscillations of the glycolytic pathway in muscle extracts. *J. Biol. Chem.* 249:3241–3247.
 46. Yaney, G. C., V. Schultz, B. A. Cunningham, G. A. Dunaway, B. E. Corkey, et al. 1995. Phosphofructokinase isozymes in pancreatic islets and clonal β -cells (INS-1). *Am. J. Physiol.* 44:E1285–E1289.
 47. Ma, Z., S. Ramanadham, K. Kempe, Z. Hu, J. Ladenson, et al. 1996. Characterization of expression of phosphofructokinase isoforms in isolated rat pancreatic islets and purified β -cells and cloning and expression of the rat phosphofructokinase-A isoform. *Biochim. Biophys. Acta.* 1308:151–163.
 48. Zhang, M., B. Fendler, B. Peercy, P. Goel, R. Bertram, et al. 2008. Long lasting synchronization of calcium oscillations by cholinergic stimulation in isolated pancreatic islets. *Biophys. J.* 95:467–468.
 49. Grapengiesser, E., H. Dansk, and B. Hellman. 2004. Pulses of external ATP aid to the synchronization of pancreatic β -cells by generating premature Ca^{2+} oscillations. *Biochem. Pharmacol.* 68:667–674.
 50. Hellman, B., H. Dansk, and E. Grapengiesser. 2004. Pancreatic β -cells communicate via intermittent release of ATP. *Am. J. Physiol.* 286:E759–E765.
 51. Smolen, P. 1995. A model for glycolytic oscillations based on skeletal muscle phosphofructokinase kinetics. *J. Theor. Biol.* 174:137–148.
 52. Li, Y.-X., and J. Rinzel. 1994. Equations for InsP3 receptor-mediated $[\text{Ca}^{2+}]_i$ oscillations derived from a detailed kinetic model: a Hodgkin-Huxley like formalism. *J. Theor. Biol.* 166:461–473.
 53. Ashcroft, F. M., D. E. Harrison, and S. J. H. Ashcroft. 1984. Glucose induces closure of single potassium channels in isolated rat pancreatic β -cells. *Nature.* 312:446–448.
 54. Henquin, J.-C. 1988. ATP-sensitive K^+ channels may control glucose-induced electrical activity in pancreatic β -cells. *Biochem. Biophys. Res. Commun.* 156:769–775.
 55. Ermentrout, G. B. 2002. Simulating, Analyzing, and Animating Dynamical Systems: A Guide to XPPAUT for Researchers and Students. SIAM, Philadelphia, PA.
 56. Frigo, M., and S. G. Johnson. 2005. The design and implementation of FFTW3. *Proc. IEEE.* 93:216–231.
 57. Mao, C. S., N. Berman, K. Roberts, and E. Ipp. 1999. Glucose entrainment of high-frequency plasma insulin oscillations in control and type 2 diabetic subjects. *Diabetes.* 48:714–721.
 58. Stagner, J. I., and E. Samols. 1985. Role of intrapancreatic ganglia in regulation of periodic insular secretions. *Am. J. Physiol.* 248:E522–E530.
 59. Matthews, D. R., D. A. Lang, M. A. Burnett, and R. C. Turner. 1983. Control of pulsatile insulin secretion in man. *Diabetologia.* 24:231–237.
 60. Stagner, J. I., and E. Samols. 1985. Perturbation of insulin oscillations by nerve blockade in the in vitro canine pancreas. *Am. J. Physiol.* 248:E516–E521.
 61. Stagner, J. I., and E. Samols. 1986. Modulation of insulin secretion by pancreatic ganglionic nicotinic receptors. *Diabetes.* 35:849–854.
 62. Gilon, P., and J.-C. Henquin. 2001. Mechanisms and physiological significance of the cholinergic control of pancreatic β -cell function. *Endocr. Rev.* 22:565–604.
 63. Zarkovic, M., and J.-C. Henquin. 2004. Synchronization and entrainment of cytoplasmic Ca^{2+} oscillations in cell clusters prepared from single or multiple mouse pancreatic islets. *Am. J. Physiol.* 287:E340–E347.
 64. Salehi, A., S. S. Quader, E. Grapengiesser, and B. Hellman. 2005. Inhibition of purinoceptors amplifies glucose-stimulated insulin release with removal of its pulsatility. *Diabetes.* 54:2126–2131.